Journal of Applied Electrochemistry **32**: 225–230, 2002.

Initial stages of tin electrodeposition from sulfate baths in the presence of gluconate

J. TORRENT-BURGUÉS[1]*, E. GUAUS[1] and F. SANZ[2]
[1]*Dep. d'Enginyeria Química, Univ. Politècnica de Catalunya, C/Colom 1, 08222-Terrassa, Spain*
[2]*Dep. de Química Física, Univ. de Barcelona, C/Martí i Franquès 1, 08028-Barcelona, Spain*
*(*author for correspondence, fax: +34 93 7398301, e-mail: jtorrent@eq.upc.es)*

Received 17 January 2001; accepted in revised form 28 November 2001

Key words: deposit morphology, gluconate, nucleation, sulfate bath, tin electrodeposition

Abstract

Tin electrodeposition in its initial stages in acid sulfate/gluconate baths was studied with varying tin and gluconate concentrations using potential-controlled electrochemical techniques. The deposit morphology was observed by scanning electron microscopy (SEM). A comparison with tin electrodeposition from acid sulfate baths in the absence of gluconate was also carried out. Use of a highly acidic bath leads to nonuniform deposits, even in the presence of gluconate; at pH 4 deposits are uniform, brilliant and suitable for finishing applications. Tin crystallites have a well defined morphology which depends on bath agitation conditions. In the absence of agitation, the crystallites have the same tetragonal shape as in a sulfate bath without gluconate.

1. Introduction

Tin has been industrially applied as a coating on a large number of metals, particularly steel (tinplate), to impart corrosion resistance, enhance appearance or improve solderability. Although the use of electrodeposited tin is not new, there is increasing interest in its use as a substitute for conventional coatings because tin baths have much less environmental impact. As examples, tin and tin alloys are possible candidates to substitute toxic chromium and cadmium deposits used for decorative and electrical/electronic applications, respectively [1–3]. Also, pure electroplated tin has been used in microelectronics as an alternative for tin/lead finishes [4].

Tin has been commercially electrodeposited from several acid and alkaline baths [5–8]. Recently published studies on tin and tin-alloy electrodeposition [8–16] focus mainly on the influence of either additives, bath composition or plating variables to obtain coatings for commercial applications; only a few studies focus on the reduction kinetics of Sn(II) by chronoamperometric techniques [17, 18]. On the one hand, some of the reports [9, 10, 16] show that the use of sulfate/gluconate baths is a promising alternative. On the other hand, gluconate is reported to be useful as a complexing agent and as inhibitor against corrosion [19 and references cited therein].

In this work we study the initial stages of tin electrodeposition from highly acidic and pH 4 sulfate/gluconate baths using dilute solutions and a vitreous carbon electrode. The electrodeposition is carried out under controlled potential and studied using several electrochemical techniques (voltammetry, stripping, and chronoamperometry). The structure of the deposits is analysed by scanning electron microscopy (SEM) and the observed morphology of tin crystallites is compared with that obtained in sulphate baths without gluconate [20].

2. Experimental details

The electrochemical measurements were performed in a three-electrode cell using vitreous carbon as working electrode (0.031 cm^2), a platinum wire as counter electrode and Ag/AgCl/KCl (3 M) as reference electrode, inserted in a Luggin capillary. All potentials are referred to this electrode. An Autolab PSTAT10 was used as potentiostat, controlled by a microcomputer. Different sets of voltammetric, chronoamperometric and stripping experiments were performed. Voltammetric experiments were carried out at 50 mV s^{-1}, scanning at first to negative potentials, and running only one cycle in each experiment. The initial potential was −0.1 V, which almost coincides with the open circuit potential. Stripping analysis was always performed immediately after potentiostatic deposition without removing the electrode from the cell. Potentiodynamic stripping was always carried out using an initial potential at which deposition did not occur and at a scan rate of 50 mV s^{-1}. Chronoamperometric experiments were carried out stepping from an initial potential of −200 mV to a wide range of selected final potentials.

After electrochemical deposition of tin, the surface was removed from the plating solution and rinsed with

Millipore pure water. The deposit morphology was examined using a Hitachi S2300 scanning electron microscope.

Chemicals used were $SnSO_4$, sodium gluconate ($NaC_6H_{11}O_7$), sulfuric acid and Na_2SO_4 (analytical grade). All solutions were freshly prepared with water, first distilled and then treated with a Milipore Milli Q system. The gluconate/sulfate bath contained 0.01 or 0.016 M $SnSO_4$, 0.2–1 M Na_2SO_4 as supporting electrolyte and 0.06–0.2 M sodium gluconate as chelating agent, and the pH was adjusted to 4. In addition, a highly acidic sulfate/gluconate bath was studied which contained 0.01 M $SnSO_4$, 1 M H_2SO_4 and 0.06 M sodium gluconate. Before each experiment the solution was deaerated with argon. The working electrode was polished mechanically before each run with 3.75 and 1.87 μm alumina powder followed by a short electrochemical conditioning.

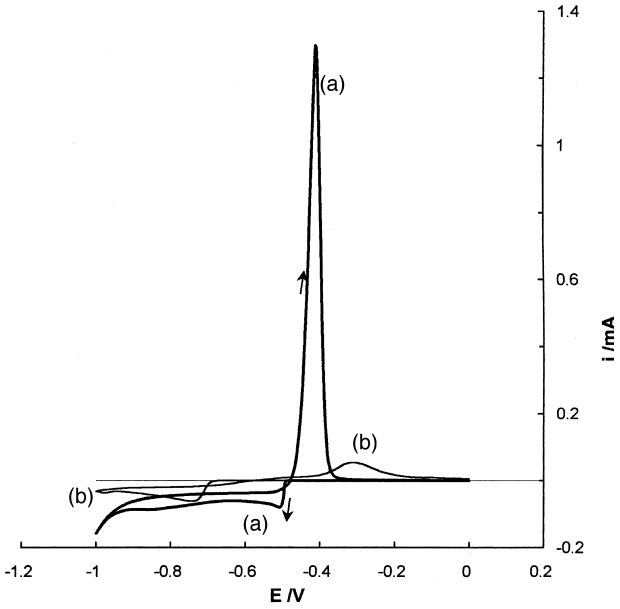

Fig. 1. Cyclic voltammograms at 50 mV s^{-1} for solutions: (thick line (a)) 0.01 M $SnSO_4$, 1 M sulfuric acid, 0.06 M sodium gluconate; (thin line (b)) 0.01 M $SnSO_4$, 1 M Na_2SO_4, 0.06 M sodium gluconate, pH 4. Arrows indicate the scan direction.

3. Results and discussion

3.1. *Voltammetric results*

Figure 1 shows the voltammetric response of tin electrodeposition in an acid sulfate/gluconate bath. The voltammogram at highly acidic solution (curve (a)) was compared with that reported for tin sulfate in sulfuric acid [20] and no significant influence of gluconate was observed. This is due to the fact that in highly acidic solutions, gluconate is in the form of gluconic acid and therefore no complexing action by the gluconate anion is possible with tin cations. For the sulfate/gluconate bath at pH 4 (curve (b)), the tin reduction potential shifts to more negative values, from around −500 mV to around −700 mV, due to the stability of tin–gluconate complexes in solution (log $K_1 = 3.01$, log $K_2 = 2.28$, at $I = 0.1$ mol dm^{-3} and 20 °C [21]). Reversing the potential on reaching the reduction peak, the response shows the expected behaviour for an electrodeposition process, which is a loop with a cathodic current greater than that recorded during the cathodic potential scan. Voltammetric curves at pH 4 also show, as expected, that the hydrogen evolution shifts to more negative potentials, a situation which can not be obtained in the absence of gluconate. Even so, the calculated charges from the voltammetric curves with a cathodic potential limit of −1 V show that Q_- is slightly larger than Q_+, indicating that a small hydrogen evolution occurs.

In the oxidation scan at pH 4 (Figure 1, curve (b)) two peaks appear between −500 and −300 mV instead of the single peak, at around −400 mV, observed either in the absence of gluconate [20] or with gluconate (Figure 1, curve (a)) using highly acidic sulphate baths. Figure 2

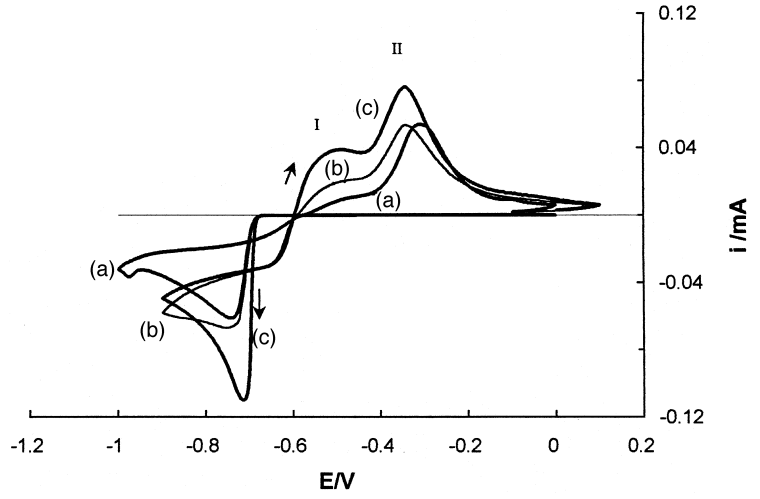

Fig. 2. Cyclic voltammograms at 50 mV s^{-1} for solutions 0.01 M $SnSO_4$, 0.8 M Na_2SO_4, y M sodium gluconate, pH 4: (thick line (a)) $y = 0.06$, (thin line (b)) $y = 0.12$, (thick line (c)) $y = 0.20$. Arrows indicate the scan direction.

shows both peaks in a more detailed form with varying gluconate concentrations. Increasing the gluconate concentration does not lead to a significant influence on the reduction peak potential, but a sharper rise is observed, which will be discussed together with the chronoamperometric results. In the first oxidation peak (peak I), the influence is significant because the peak increases with gluconate concentration. More relevant is the height ratio between peak I and peak II. Thus, the ratios (i_p(I)/i_p(II)) measured in Figure 2 are 0.21, 0.37 and 0.51 for gluconate concentrations of 0.06 (curve (a)), 0.12 (curve (b)) and 0.20 M (curve (c)), respectively.

Figure 3 shows the voltammetric response for two different tin solution concentrations. Increasing concentration produces a stronger reduction peak, which shifts slightly to more positive potentials. In the oxidation scan, the first peak is practically unchanged with varying tin concentration, however the second peak increases. The height ratios of peak I to peak II are 0.25 and 0.37 for tin concentrations of 0.016 (curve (b)) and 0.01 M (curve (a)), respectively. No significant influence of ionic strength was observed.

It is clear that the first oxidation peak is related to the complexing action of gluconate on tin ions produced during the oxidation process, and hence depends on the gluconate concentration. This conclusion is also confirmed by the fact that voltammetric curves obtained at very low scan rates (2 mV s^{-1}) show a much higher current increase for the first oxidation peak, because the depletion of the gluconate diffusion layer to the electrode is less.

3.2. *Stripping analysis*

Stripping experiments were made at several potentials and two deposition times (10 and 20 s) were considered. Figure 4 shows that the highly acidic sulfate/gluconate bath only presents one stripping oxidation peak (curve a), as obtained in the voltammogram. Figure 4 also

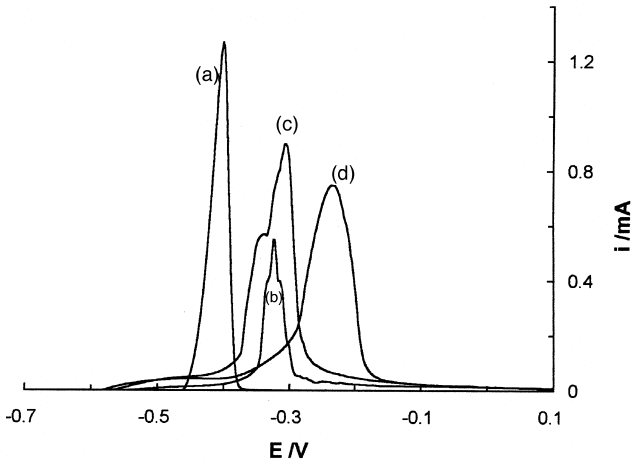

Fig. 4. Stripping voltammograms at 50 mV s^{-1} of deposits obtained potentiostatically with agitation: from a 0.01 M $SnSO_4$, 1 M sulfuric acid, 0.06 M sodium gluconate solution for 10 s at −600 mV (curve (a)); and from 0.01 M Sn, 0.8 M Na_2SO_4, x M gluconate, pH 4 solutions for 10 s at −750 mV (curve (b): $x = 0.06$, curve (c): $x = 0.12$, curve (d): $x = 0.2$).

shows strippings for different gluconate concentration baths at pH 4 (curves (b)–(d)). In this case, the strippings present a first oxidation peak which is smaller than the second, similar to those obtained in the voltammogram.

The influence of gluconate concentration is demonstrated by the significance of the first oxidation peak. The first peak is lower when the gluconate concentration is lower, but also a shift of the second peak to more positive potentials is observed for the higher gluconate concentration. It can also be seen that at low deposition times (10 s) this second peak is really a double peak, but at higher deposition times (20 s) it appears as a single one.

3.3. *Chronoamperometric curves*

Several chronoamperometric experiments were performed for various tin and gluconate concentrations, using a wide range of applied potentials. These exper-

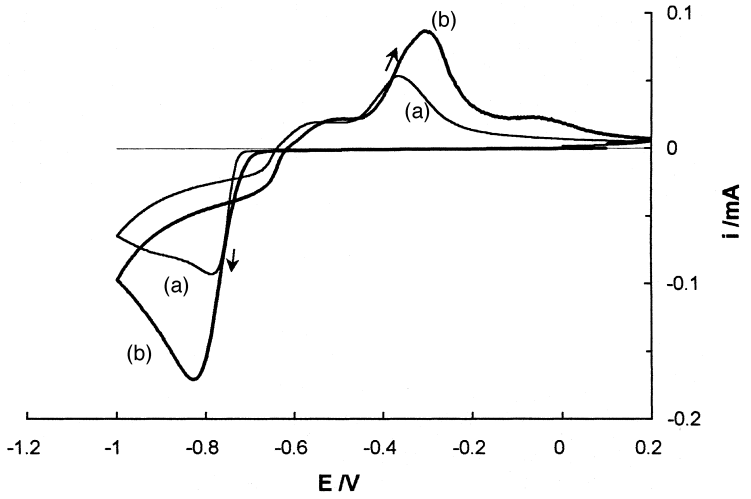

Fig. 3. Cyclic voltammograms at 50 mV s^{-1} for solutions x M $SnSO_4$, 0.8 M Na_2SO_4, 0.12 M sodium gluconate, pH 4: (thin line (a)) $x = 0.01$, (thick line (b)) $x = 0.016$. Arrows indicate the scan direction.

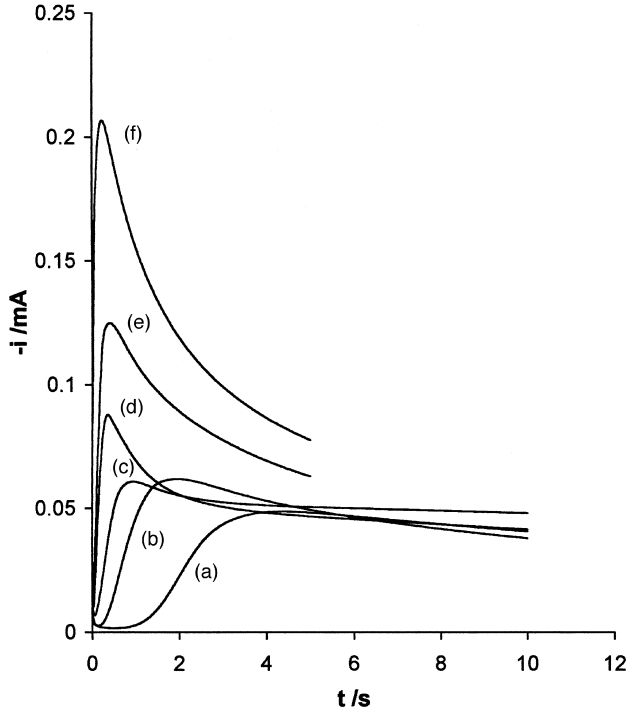

Fig. 5. Potentiostatic transients for solution 0.01 M $SnSO_4$, 0.8 M Na_2SO_4, 0.12 M sodium gluconate, pH 4. The potential step transients were made from $E_0 = -200$ mV to: (a) −675, (b) −700, (c) −750, (d) −775, (e) −800 and (f) −900 mV.

iments indicate that the electrodeposition process is dependent on gluconate concentration. The i/t curve rise is sharper when gluconate concentration increases, and is similar to that observed in the reduction peak of voltammograms. Figure 5 shows the chronoamperometric curves for sulfate/gluconate solutions at pH 4 with tin and gluconate concentrations of 0.01 and 0.12 M, respectively.

The theoretical analysis of chronoamperometric curves was carried out by subtracting the induction time, t_0, something which is essential for correct analysis, especially at lower overpotentials. As is well known, the chronoamperometric curves show several sections allowing several lengths of time dependence. Usually there is a wider section on the rising part which is chosen for process analysis. The analysis of this section shows that the current basically has a linear dependence with t (Figure 6), indicating that electrodeposition proceeds through an instantaneous nucleation with 2D growth control at low (0.06 M) and medium (0.12 M) gluconate concentrations and at not very high or very low overpotentials. Gómez et al. [20] reported instantaneous nucleation with 3D growth controlled by diffusion for the electrodeposition of tin in highly acidic nongluconated sulphate baths. Consequently, gluconate has an important effect during the initial stages of tin electrodeposition.

When experiments are performed at high overpotentials, a change is observed in the mechanism to diffusion control (i depends on $t^{1/2}$). This diffusion control is suppressed when tin concentration is increased, with the linear dependence of i against t again appearing. On the

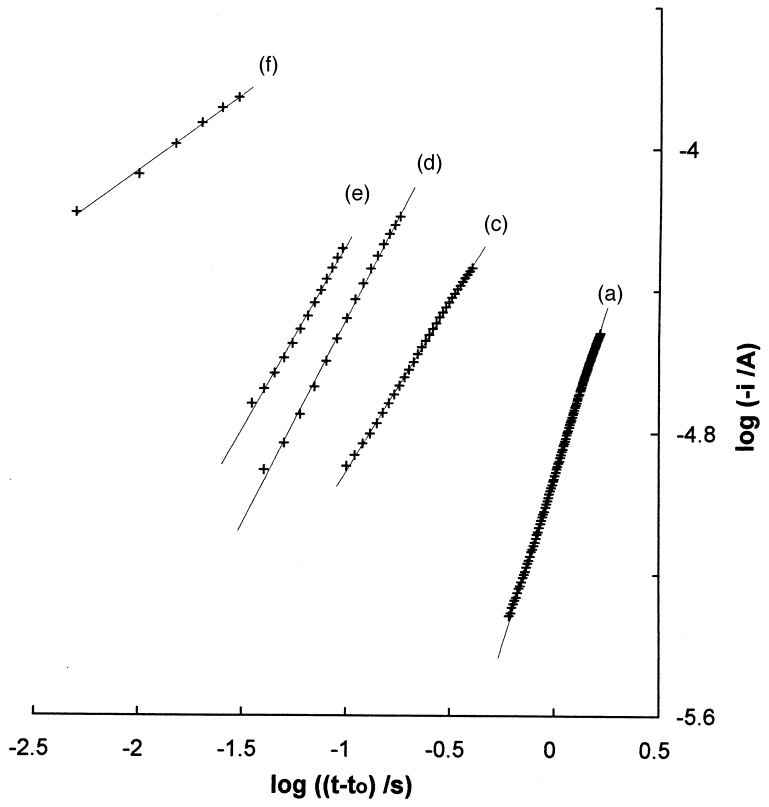

Fig. 6. Plot of log i against log $(t-t_0)$ for the curves of Figure 5.

other hand, experiments at very low overpotentials show a t^2 dependence of the current on time, so describing progressive nucleation with 2D growth control. These changes in the current time dependence with applied potential are usual in electrodeposition processes. Higher overpotentials favour instantaneous nucleation instead of progressive, as occurs at lower overpotentials.

Experiments performed at a higher gluconate concentration (0.2 M) show a change in the electrodeposition mechanism. Under these conditions it has been observed that the current depends on t^2 at low and also medium overpotentials. Then, progressive nucleation with 2D growth and fast diffusion occurs. Although this dependence can also be assigned to instantaneous nucleation with 3D growth and fast diffusion, the presence of a maximum on i/t curves indicates evidence of a 2D mechanism. This change in mechanism could explain the differences observed in the rise of the reduction peaks on both the chronoamperometric and voltammetric curves as gluconate concentration increases. At high overpotentials, the current depends linearly on t, and then the assigned mechanism, for low and medium gluconate concentration, again comes into play.

Higher gluconate concentrations favour progressive nucleation, and this fact may be attributed to a blocking effect of gluconate molecules adsorbed on a certain fraction of the active surface sites. Also, the presence of gluconate favours the occurrence of a 2D instead of a 3D process, with the 3D process being the most usual in electrodeposition in the absence of additives.

3.4. *SEM micrographs*

Figure 7 shows the SEM micrographs obtained under different electrodeposition conditions. Figure 7(a) shows that nonuniform deposits were obtained from the highly acidic sulfate/gluconate bath, and Figure 7(b) shows a uniform grain and more brilliant deposit obtained at a pH 4 sulfate/gluconate bath. Figure 7(c) shows an enlargement of Figure 7(b) that reveals the size and shape of the tin crystallites. Tetragonal and cubic morphologies are observed, and some of the crystallites are also observed beginning to coalesce.

Figure 8 shows two deposits obtained at low charges, one of them (a) without agitation and the other (b) with agitation. Under agitation conditions, tin crystallites present both cubic and tetragonal morphologies (mean size $\sim 0.34\,\mu m \times 0.34\,\mu m \times 0.34\,\mu m$ and $\sim 0.14\,\mu m \times 0.14\,\mu m \times 0.34\,\mu m$ respectively). Without agitation the crystallites are predominantly tetragonal (mean size $\sim 0.17\,\mu m \times 0.17\,\mu m \times 0.61\,\mu m$), and in accordance with the morphology reported in the absence of gluconate [20].

The crystallite size observed in Figure 8(a) is practically the same, a fact that indicates instantaneous nucleation. Even if a direct correlation of chronoamperometric analysis with the SEM results cannot be established because the SEM electrodeposits are obtained at much longer times, the SEM observation is coherent with the chronoamperometric analysis. The measured number of crystallites per unit area in Figure 8(a) is 1.5×10^7 cm^{-2} and the mean crystal growth rate of tetragonal crystallites is $\sim 2.3 \times 2.3 \times 8.2$ nm s^{-1}. The measured number of crystallites per unit area in Figure 8(b) is 1.4×10^8 cm^{-2} and the mean crystal growth rate of tetragonal crystallites is $\sim 2.8 \times 2.8 \times 6.8$ nm s^{-1}, while that of the cubic crystallites is ~ 6.8 nm s^{-1}. Thus, we can conclude that electrodeposition without agitation favours the growth of tetragonal crystallites along the c axes.

We can now, compare the crystallite surface density measured in Figure 8(a), 1.5×10^7 cm^{-2}, with the value

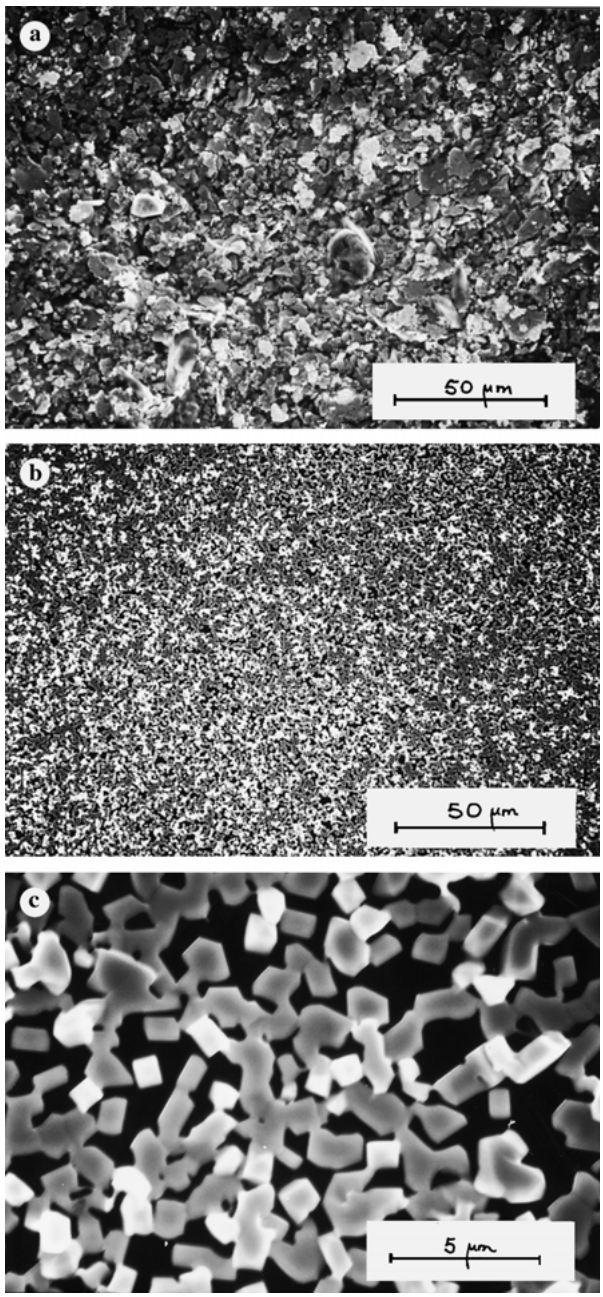

Fig. 7. SEM micrographs of tin electrodeposits obtained with agitation: (a) 0.01 M $SnSO_4$, 1 M sulfuric acid, 0.06 M sodium gluconate solution for 100 s at −530 mV; and (b, c) 0.01 M $SnSO_4$, 0.8 M Na_2SO_4, 0.06 M sodium gluconate solution, pH 4, for 300 s at −680 mV.

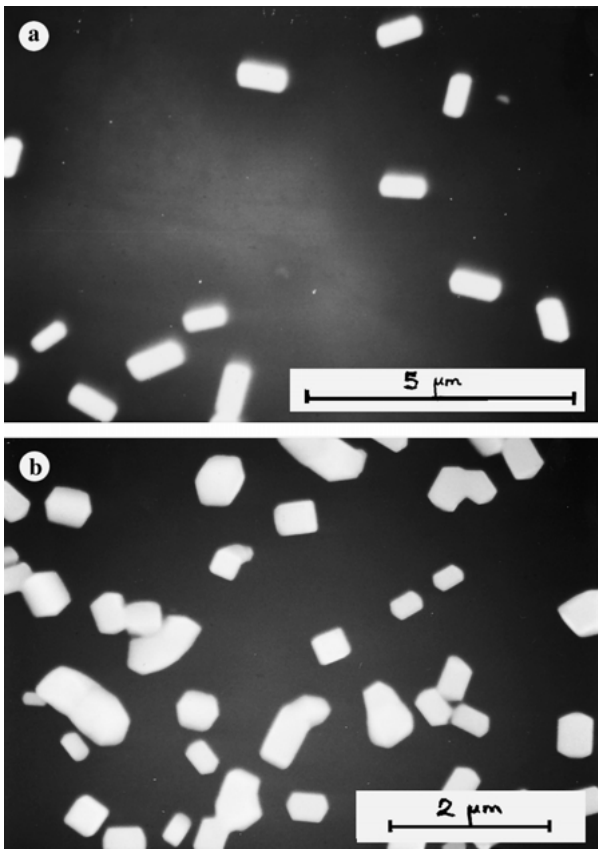

Fig. 8. SEM micrographs of tin electrodeposits obtained with a 0.01 M $SnSO_4$, 0.8 M Na_2SO_4, 0.06 M sodium gluconate solution, pH 4: (a) without agitation for 75 s at −625 mV; and (b) with agitation for 50 s at −680 mV.

reported by Gómez et al. [20] at a similar overpotential, but without gluconate, which is 1.3×10^5 cm^{-2}. We observe that gluconate favours nucleation in the initial stages of the process, and this result explains the observed behaviour in chronoamperometric experiments, where the rise of the i/t curves is sharper as the gluconate concentration increases. But, by comparing the growth rate value along the c axis measured in Figure 8(a), 8.2 nm s^{-1}, with that reported by Gómez et al. [20], 90 nm s^{-1}, we can conclude that gluconate inhibits the growth rate. This fact permits better control of tin crystallite growth and leads to more uniform deposits.

4. Conclusions

The use of a sulfate/gluconate bath at pH 4 shifts the tin electrodeposition process to more negative potentials. The deposits are uniform, in contrast to those obtained in a highly acidic bath, revealing the potential of sulfate/gluconate baths at pH 4 for electrodeposited tin finishes. The deposit morphology shows that tetragonal tin crystallites are obtained without agitation, but that this favours the development of cubic crystallites. When comparing similar overpotentials in baths with and without gluconate, gluconate is observed to favour the nucleation of tin but to decrease the growth rate of tin crystallites.

Experiments, performed under varying conditions of tin and gluconate concentrations, reveal the influence of these factors in the electrodeposition process. The electrodeposition process at the initial stages proceeds via instantaneous nucleation with a 2D growth control, but the presence of higher gluconate concentrations favours a change in the electrodeposition mechanism towards progressive nucleation with 2D growth control.

Acknowledgements

We would like to express our thanks to the Serveis Científico-Tècnics of the Universitat de Barcelona for their technical support in SEM images. This work was supported by grants from the Universitat Politècnica de Catalunya and the CICYT MAT 97-0379 project (Spain).

References

1. K.N. Strafford and A. Reed, 'Coatings and Surface Treatment for Corrosion and Wear Resistance' (1984), p. 74.
2. R. Sabitha, Malathy Pushpavanam, M. Mahesh Sujatha and T. Vasudevan, *Trans. Met. Finish. Ass. of India* **5** (1996) 267.
3. M. Degrez and R. Winand, Conference: Second Congress Metallurgy and Uses, Pub. Cobalt Development Institute (1986), p. 432.
4. K.G. Sheppard, Abstracts of the 190th Meeting of The Electrochemical Society, Vol. 96-2, no. 306 (The Electrochemical Society, Pennington, NJ, 1996), p. 395.
5. K. Othmer, 'Encyclopedia of Chemical Technology', Vol. 24 (4th ed. Wiley, New York, 1997), p. 105.
6. D.J. Maykuth and W.B. Hampshire, 'ASM Metals Handbook', Vol. 13, (9th edn, ASM Publications, 1998), p. 770.
7. B.N. Stirrup and N.A. Hampson, *J. Electroanal. Chem.* **5** (1997) 429.
8. M.I. Smirnov, K.M. Tyutina and A.N. Popov, *Russian J. Electrochem.* **31** (1995) 498.
9. V.S. Vasantha, Malathy Pushpavanam and V.S. Muralidharan, *Met. Finish.* **93** (1995) 16.
10. T. Sonoda, H. Nawafume and S. Mizumoto, *Plat. Surf. Finish.* **79** (1992) 78.
11. A. Aragon, M.G. Figueroa, R.E. Gana and J.H. Zagal, *J. Appl. Electrochem.* **22** (1992) 558.
12. N. Kaneko, N. Shinohara and H. Nezu, *Electrochim. Acta* **37** (1992) 2403.
13. G.S. Tzeng, S.H. Lin, Y.Y. Wang and C.C. Wan, *J. Appl. Electrochem.* **26** (1996) 419.
14. V.S. Vasantha, Malathy Pushpavanam, P. Kanaraj and V.S. Muralidharan, *Trans. Inst. Met. Finish.* **74** (1996) 28.
15. Malathy Pushpavanam, M. Mahesh Sujatha and T. Vasnderan, *Trans. Met. Finish. Ass., India* **5** (1996) 267.
16. S.S. Abd el Rehim, S.A. Refaey, G. Schwitzgebel, F. Taha and M.B. Saleh, *J. Appl. Electrochem.* **26** (1996) 413.
17. C.J. Van Velzen, M. Sluyters-Rehbach and J.H. Sluyters, *Electrochim. Acta* **32** (1987) 815.
18. J. Wijenberg, 'Initial Stages of Electrochemical Phase Formation', PhD thesis (University of Utrech, The Netherlands, 1991), chapter 6.
19. S.A.M. Refaey, *Appl. Surf. Sci.* **157** (2000) 199.
20. E. Gomez, E. Guaus, F. Sanz and E. Valles, *J. Electroanal. Chem.* **465** (1999) 63.
21. T.N. Maksin, B.Z. Zmbova and D.S. Veselinovic, *J. Serb. Chem. Soc.* **56** (1991) 337.